

A Study on “Bottleneck” Phenomenon during Parachute Inflation

Sol Song Pak*, Chol Min Ri, Won Hak Kim, Nam Song Pak and Hyong Gyu Jon

Faculty of dynamics, Kim Il Sung University, Pyongyang, Democratic People’s Republic of Korea

*Corresponding author: Sol Song Pak, Faculty of Dynamics, Kim Il Sung University, Pyongyang, Democratic People’s Republic of Korea, E-mail: GI.Li803@star-co.net.kp

Received date: 1-June-2023, Manuscript No. tspa-23-104931; **Editor assigned:** 03-June-2023, Pre-QC No. tspa-23-104931 (PQ); **Reviewed:** 10-July-2023, QC No. tspa-23-104931 (Q); **Revised:** 12-July-2023, Manuscript No. tspa-23-104931 (R); **Published:** 30-July-2023, DOI. 10.37532/2320-6756.2023.11(7).361

Abstract

In this paper we focus on Fluid–Structure Interaction (FSI) modeling and performance analysis of the large-scale parachutes to be used with the spacecraft. We address the computational challenges with the latest techniques developed by the TAFSM (Team for Advanced Flow Simulation and Modeling) in conjunction with the SSTFSI (Stabilized Space–Time Fluid–Structure Interaction) technique. The Arbitrary Lagrangian Eulerian (ALE) Method-a Fluid-Structure Interaction (FSI) model, was used to simulate the inflation process of a main parachute (a ring sail parachute, which was used in manned spacecraft) in an infinite mass situation. The dynamic relationship between canopy shape and flow field was obtained and the adverse inflation phenomena such as asymmetric inflation and whip were observed in simulation results. The “bottleneck” phenomenon in inflation process was found and verified by physical tests. Based on the analysis of calculation results, it is found that the large canopy area, the complicated canopy structure or high inflation speed can block the air mass into the parachute, which can cause the “Bottleneck” phenomenon. But the necessary occurrence conditions of the phenomenon need to be studied in future. The present work is significant for explaining parachute working mechanism and preventing its failure. In this paper we discussed a method to prevent “Bottleneck” phenomenon in the case of the large-scale parachute.

Keywords: Parachute; Inflating process; Fluid–structure interaction; Design configurations; Arbitrary Lagrangian Eulerian

Introduction

Various types of Fluid-Structure Interaction (FSI) problems have been addressed and numerous FSI solution techniques have been developed in recent decades [1-4]. The Team for Advanced Flow Simulation and Modeling (TAFSM) has addressed many of the challenges involved in FSI modeling of parachutes [5-7], with parallel, 3D computations going as far back as 2000. The TAFSM research on parachute FSI modeling and FSI modeling in general, has been a part of the FSI research emphasis we have seen in recent decades in computational engineering and science [1-3, 8-10]. The quasi-direct FSI coupling technique was introduced in [11, 12] and became part of the core technology used in the subsequent parachute FSI simulations of the TAFSM [13-20]. Large parachutes are made of a large number of gores, where a gore can be seen as the slice of the canopy between two radial reinforcement cables running from the parachute vent to the skirt. Ring-sail parachute gores are constructed from ‘rings’ and ‘sails’, resulting in a parachute canopy with hundreds of gaps and slits.

Citation: Pak S S, Ri C M, Kim W H, *et al.* A Study on “Bottleneck” Phenomenon during Parachute Inflation. J. Phys. Astron.2023;11(7):361.

©2023 Trade Science Inc.

The complexity created by this geometric porosity makes FSI modeling inherently challenging. Historically based on experimental data, the parachute evaluation often requires numerous flight tests, which can prove expensive and time consuming, and which do not always permit to reach a good understanding of the parachute dynamic behavior.

Numerical results including opening load, drag characteristics, swinging angle, etc. are well consistent with wind tunnel tests.

In addition, this coupled method can get more space–time detailed information such as geometry shape, structure, motion, and flow field.

Compared with previous inflation time method, this method is a completely theoretical analysis approach without relying on empirical coefficients, which can provide a reference for material selection, performance optimization during parachute design.

This paper describes the simulation of the “bottle neck” phenomena in general circular parachute inflation process and a method to prevent this phenomena.

The numerical models were developed to replicate a series of parachute drop tests conducted in the early 1950s. Wright Air Development Division Report AFTR 5867 documents 700 parachute drop tests, using twenty seven different parachutes, at the Goodyear Aircraft Corporation airship dock in Akron, Ohio between 1952 and 1954.

The data from these tests were compiled into charts and referenced in the Parachute Recovery Systems Design Manual (T.W. Knacke).

The numerical models were developed using Fluid Structure Interaction (FSI) techniques in the commercially available transient dynamic finite element code LS-DYNA.

This paper describes the “Bottle neck” phenomena happening in an 18.81m Nominal Diameter (D0) 10% extended skirt parachute model.

The techniques for building a consistent starting condition are described in Section 2. Parachute test data are described in section 3.

The parachute simulation techniques are described in Section 4. Results from the simulation are reported in Section 5. We give our concluding remarks in Section 6.

Starting Condition

A consistent starting condition is essential for making accurate comparisons in many applications using FSI modeling. Starting conditions are especially important when investigating the unsteady features. A number of techniques for building FSI starting conditions are reported in [8, 9]. These techniques mostly focus on starting the FSI computations softly. The purpose of further improving the starting condition with the methods introduced here is primarily related to making the starting conditions consistent and matching what was observed during NASA drop tests. All computations reported in this paper are carried out in a parallel computing environment, using PC clusters. The meshes are partitioned to enhance the parallel efficiency of the computations. Mesh partitioning is based on the METIS algorithm. **FIG. 1** shows, for a parachute, the canopy structure mesh and the fluid mechanics interface mesh.

The structure has 82305 nodes, 54332 four-node quadrilateral membrane elements, and 18900 two-node cable elements. There are 29 200 nodes on the canopy. The fluid mechanics interface mesh has 2140 nodes and 4180 three-node triangular elements (**FIG. 2**). We first build a starting condition for this single parachute. We begin with a parachute shape obtained with the symmetric FSI computation reported in [12]. We do another symmetric FSI computation where we specify a horizontal inflow velocity of 285.0 ft s⁻¹. After that, we generate two quadrilateral fluid mechanics meshes. With the cluster mesh, holding the parachute shapes and

positions fixed, we first do a fluid mechanics computation using the semi-discrete formulation given in [17]. The inflow velocity is 285.0 ft s^{-1} . We compute 400 time steps with a time-step size of 0.174 s and seven nonlinear iterations per time step. Following that, still holding the parachute shapes and positions fixed, we do another fluid mechanics computation with the same inflow velocity. Material properties and equation of state are defined to characterize the Eulerian fluid. To simulate the fluid structure interaction, the ALE method included in LS-Dyna is used with the coupling algorithm based on the penalty method. A permeability algorithm based on Ergun law is also implemented in the coupling method. The suspension lines/risers and the fluid are not coupled in order to avoid high computational time consumption.

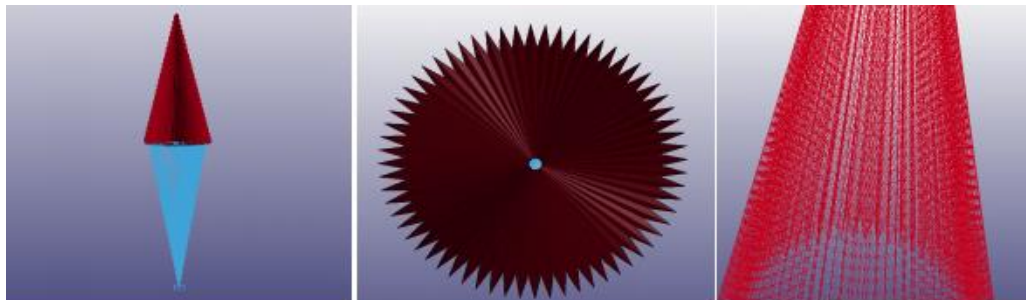


FIG. 1. Canopy structure mesh for a parachute.

The structure has 82305 nodes, 54 332 three-node triangular membrane elements, and 18900 two-node cable elements. There are 29200 nodes on the canopy.

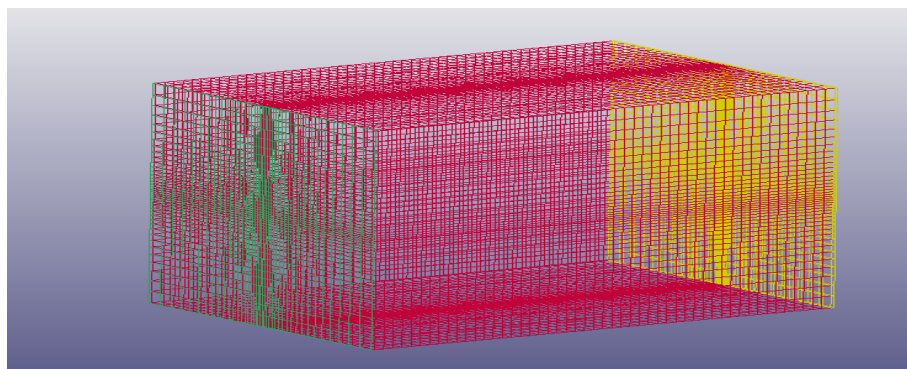


FIG. 2. Fluid mesh for a parachute.

The fluid mechanics interface mesh has 6280 nodes and 24980 four-node quadrilateral elements.

Parachute Simulation Techniques

The commercially available transient dynamic finite element code LS-DYNA was utilized to develop models for this study. The numerical approach discussed in this paper utilizes a first order Eulerian temporal solution with a second order accurate advection method. An Eulerian formulation on a Cartesian mesh is used for the fluid, Lagrangian 4-noded membrane elements based on the Belytschko-Lin-Tsay formulation for the parachute structural mesh, and a quasi-penalty based porosity coupling method was

employed to enable the two to interact. The use of an Eulerian-Lagrangian coupling algorithm permits the interaction of the fluid and structure to occur within the same computational solver and completely avoids the numerical problems associated with distortions of the fluid mesh. Following the classification discussed this coupling would be described as “partitioned” and “loose”. Partitioned meaning that the fluid and structural fields are solved separately and forces, velocities, and displacements are passed through an interface-in this case the *CONSTRAINED_LAGRANGE_IN_SOLID card, and loose meaning that the fluid and structure equations are solved once during each time-step. However, it should be noted that both the fluid and structural fields are solved within the same LS-DYNA code environment, i.e. completely separate codes are not used for this analysis. The computational model developed for this study consists of a separate parachute structural model, and a fluid model. The nodal location of the parachute apex was tracked throughout each simulation and used to measure the oscillation angle of the parachute as a function of time. This data was used to record average oscillation angle and frequency of oscillation (TABLE 1 and TABLE 2).

TABLE 1. Structural parameters.

Falling Velocity (ms ⁻¹)	Resistant area (S) (m ²) $\frac{2W}{V^2 \rho C_D}$	Nominal Diameter (D ₀) (m) $\sqrt{\frac{4S}{\pi}}$	Manufactured Diameter (D _c) (m) 0.95 D ₀	Area of Canopy (S _c) (m ²) $\frac{1}{2} \pi D_c^2$
6	277.78	18.81	16.93	450
7	204.08	16.12	15.32	368.37
8	156.25	14.1	14.1	282.03

TABLE 2. Various data.

Parameter	Value	Unit
Load mass	450	Kg
gravity	9.81	m/s ²
Air density	1.225	Kg/m ³
Falling speed	6	m/s
Coefficient	0.8	
Nominal diameter	18.81	m
Manufactured diameter	16.93	m
Area of canopy	450	m ²
Number of line	63	
Length of line	21.64	m

Simulation Results

Through the simulation, we discovered that “bottle neck” phenomenon is related to not only the size, velocity of filling air, the quality and shape of the parachute, but also the ratio of nominal diameter of the parachute and the diameter of the vent (FIG 3, to FIG. 11)

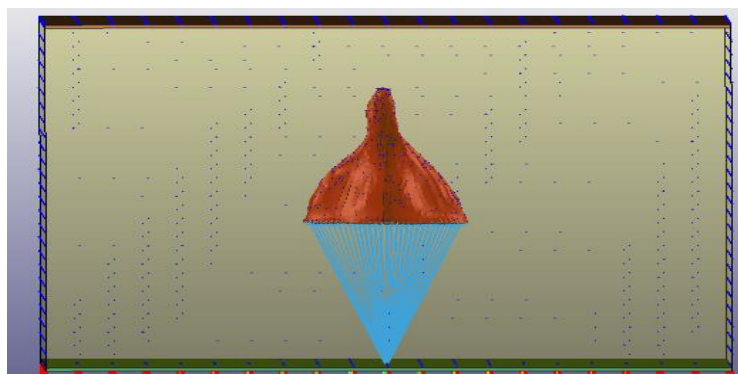


FIG. 3. A “Bottle neck” phenomenon in the case of rate of parachute nominal diameter and vent diameter is 10:1 (0.7 s).

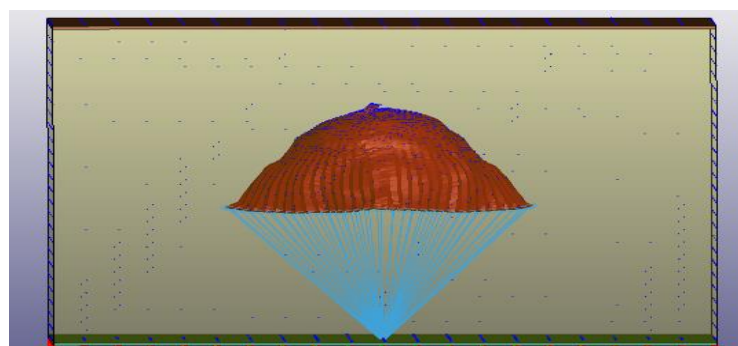


FIG. 4. A “Bottle neck” phenomenon in the case of rate of parachute nominal diameter and vent diameter is 10:1 (3.3 s).

“Bottle neck” phenomenon is observed when the ratio is 10. This phenomenon is negative to safe open of parachute. We found that “Bottle neck” phenomenon is not happened when this ratio is less than 8.

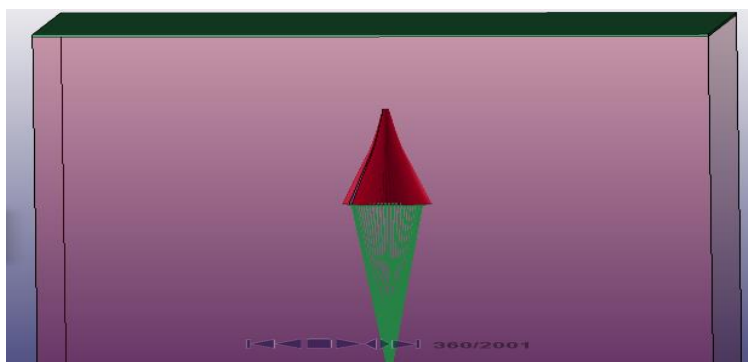


FIG. 5. Simulation of parachute in the case of rate of parachute nominal diameter and vent diameter is 8:1 (0.7 s).

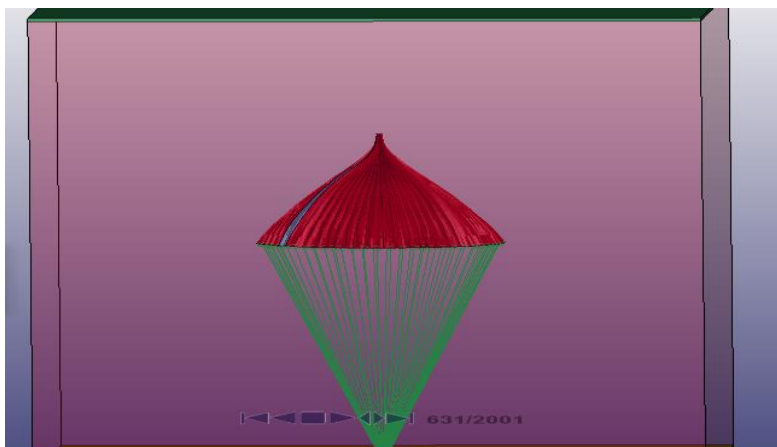


FIG. 6. Simulation of parachute in the case of rate of parachute nominal diameter and vent diameter is 8:1 (2.7 s).

As we can see the shape of parachute is nor irregular, that is, symmetry.

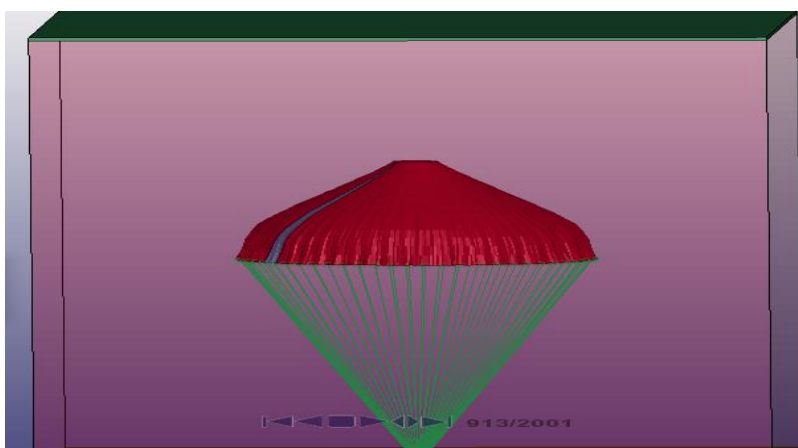


FIG. 7. Simulation of parachute in the case of rate of parachute nominal diameter and vent diameter is 8:1 (3.3 s).

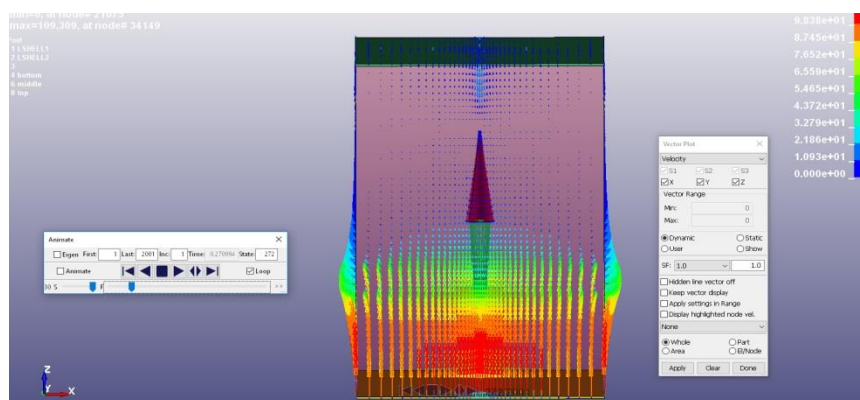


FIG. 8. Velocity vector in the case of rate of parachute nominal diameter and vent diameter is 8:1 (0.7 s).

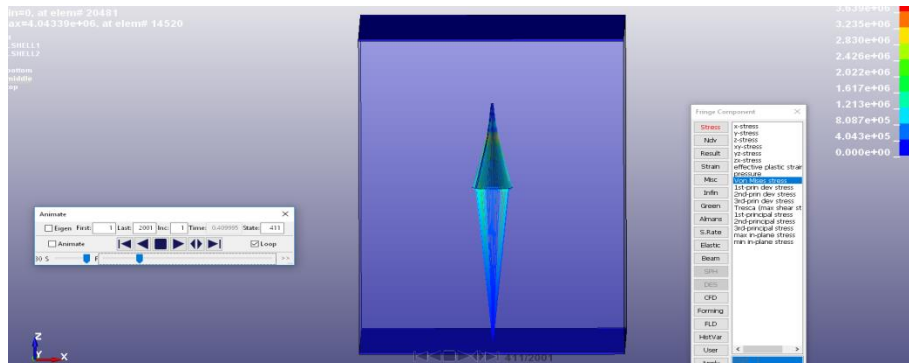


FIG. 9. Stress distributions in the case of rate of parachute nominal diameter and vent diameter is 8:1 (0.7 s).

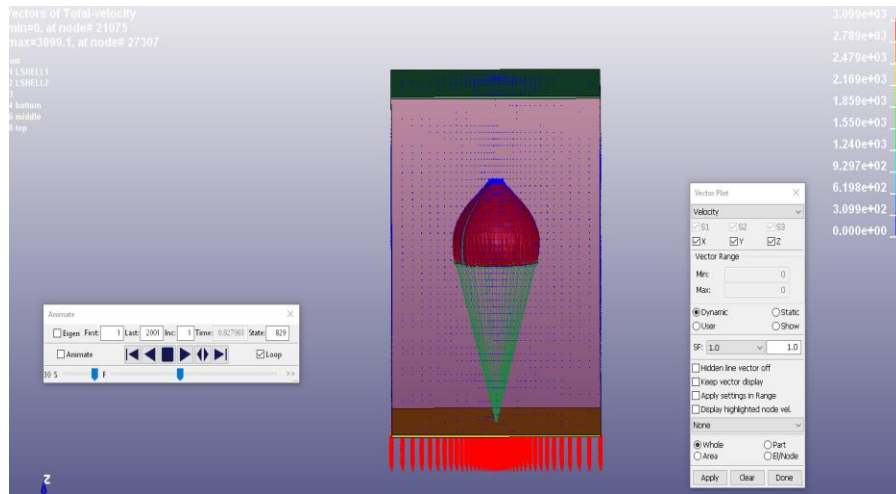


FIG. 10. Velocity vector in the case of rate of parachute nominal diameter and vent diameter is 8:1 (3.3 s).

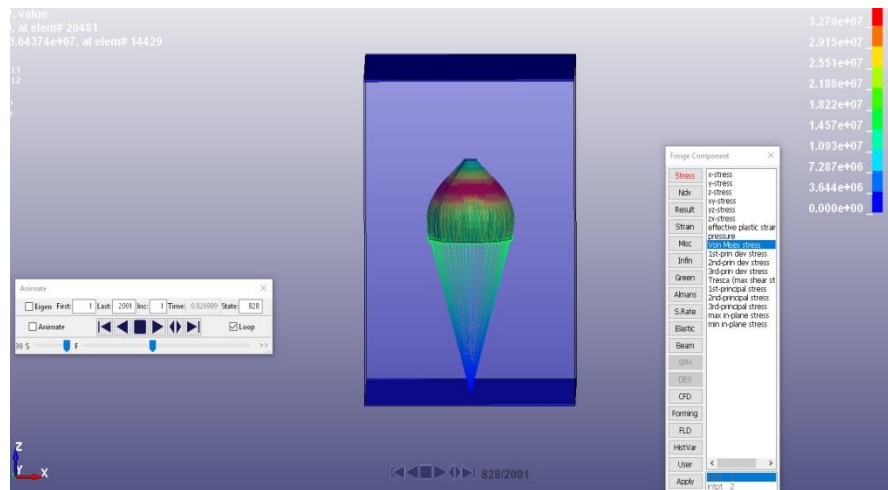


FIG. 11. Stress distributions in the case of rate of parachute nominal diameter and vent diameter is 8:1 (3.3 s).

We found that “Bottle neck” phenomenon is not happened when this ratio is less than 8. Generally, “Bottleneck” phenomenon is related to the shape of parachute, parachute material, air inlet velocity and the ratio between the diameter of vent and diameter of

nominal diameter. But the ratio between the diameter of vent and diameter of nominal diameter is considered here. We found that this ratio is affected to the “Bottleneck” phenomenon.

Conclusion

We described how we are addressing the computational challenges involved in Fluid-Structure Interaction (FSI) modeling of parachutes and “bottle neck” phenomena. We are using the Stabilized Space-Time Fluid-Structure Interaction (SSTFSI) technique together with special parachute FSI techniques developed recently in conjunction with the SSTFSI technique. We analyzed the “bottle neck” phenomenon and showed that we have a good computational capability for evaluating parachute design and performance. As a result “bottle neck” phenomenon is not happened in the case of the ratio of the nominal diameter and the vent diameter is less than 8. And other factors are affected to “Bottleneck” phenomenon. In the future we will consider that.

Acknowledgement

This study was funded by Faculty of Dynamics, Kim Il Sung University.

REFERENCES

1. Kalro V, Tezduyar TE. A parallel 3D computational method for fluid-structure interactions in parachute systems. *Comput. Methods Appl. Mech. Eng.* 2000;190(3-4):321-32.
2. Stein K, Benney R, Kalro V, et al. Parachute fluid-structure interactions: 3-D Computation. *Comput. Methods Appl. Mech. Eng.* 2000;190(3-4):373-86.
3. Tezduyar T, Osawa Y. Fluid-structure interactions of a parachute crossing the far wake of an aircraft. *Comput. Methods Appl. Mech. Eng.* 2001;191(6-7):717-26.
4. Stein K, Benney R, Tezduyar T, et al. Fluid-structure interactions of a cross parachute: numerical simulation. *Comput. Methods Appl. Mech. Eng.* 2001;191(6-7):673-87.
5. Stein KR, Benney RJ, Tezduyar TE, et al. Fluid-structure interactions of a round parachute: Modeling and simulation techniques. *J. Aircr.* 2001;38(5):800-8.
6. Stein K, Tezduyar T, Kumar V, et al. Aerodynamic interactions between parachute canopies. *J. Appl. Mech.* 2003;70(1):50-7.
7. Stein K, Tezduyar T, Benney R. Computational methods for modeling parachute systems. *Comput. Sci. Eng.* 2003;5(1):39-46.
8. Tezduyar TE, Sathe S, Keedy R, et al. Space-time finite element techniques for computation of fluid-structure interactions. *Comput. methods appl. mech. eng.* 2006;195(17-18):2002-27.
9. Tezduyar TE, Sathe S, Stein K. Solution techniques for the fully discretized equations in computation of fluid-structure interactions with the space-time formulations. *Comput. Methods Appl. Mech. Eng.* 2006;195(41-43):5743-53.
10. Tezduyar TE, Sathe S, Pausewang J, et al. Interface projection techniques for fluid-structure interaction modeling with moving-mesh methods. *Comput. Mech.* 2008;43:39-49.
11. Tezduyar TE, Sathe S, Schwaab M, et al. Fluid-structure interaction modeling of ringsail parachutes. *Comput. Mech.* 2008;43:133-42.

12. Tezduyar TE, Takizawa K, Moorman C, et al. Space–time finite element computation of complex fluid–structure interactions. *Int. J. Numer. Methods Fluids*. 2010;64(10-12):1201-18.
13. Takizawa K, Moorman C, Wright S, et al. Fluid–structure interaction modeling and performance analysis of the Orion spacecraft parachutes. *Int. J. Numer. Methods Fluids*. 2011;65(1-3):271-85.
14. Takizawa K, Moorman C, Wright S, et al. Computer modeling and analysis of the Orion spacecraft parachutes. In *Fluid Struct. Interact. II: Model. Simul. Optim.* Springer Berlin Heidelberg. 2010:53-81.
15. Hughes TJ, Liu WK, Zimmermann TK. Lagrangian-Eulerian finite element formulation for incompressible viscous flows. *Comput. methods appl. mech. eng.* 1981;29(3):329-49.
16. Tezduyar T, Aliabadi S, Behr M, et al. Parallel finite-element computation of 3D flows. *Computer*. 1993;26(10):27-36.
17. Tezduyar TE, Aliabadi SK, Behr M, et al. Massively parallel finite element simulation of compressible and incompressible flows. *Comput. Methods Appl. Mech. Eng.* 1994;119(1-2):157-77.
18. Mittal S, Tezduyar TE. Massively parallel finite element computation of incompressible flows involving fluid-body interactions. *Comput. Methods Appl. Mech. Eng.* 1994;112(1-4):253-82.
19. Mittal S, Tezduyar TE. Parallel finite element simulation of 3D incompressible flows: Fluid-structure interactions. *Int. J. Numer. Methods Fluids*. 1995;21(10):933-53.
20. Johnson AA, Tezduyar TE. Parallel computation of incompressible flows with complex geometries. *Int. J. Numer. Methods Fluids*. 1997;24(12):1321-40.